

DISTRIBUTION, STATISTICS, AND RESURFACING OF LARGE IMPACT BASINS ON MERCURY.

Caleb I. Fassett¹, James W. Head², David M. H. Baker², Clark R. Chapman³, Scott L. Murchie⁴, Gregory A. Neumann⁵, Jürgen Oberst⁶, Louise M. Prockter⁴, David E. Smith⁵, Sean C. Solomon⁷, Robert G. Strom⁸, Zhiyong Xiao^{8,9}, and Maria T. Zuber¹⁰. ¹Dept. of Astronomy, Mt. Holyoke College, South Hadley, MA 01075. ²Dept. of Geological Sciences, Brown Univ., Providence, RI 02912. ³Dept. of Space Sciences, SwRI, Boulder, CO 80302. ⁵Solar System Expl. Div. ⁴JHU/APL, Laurel, MD 20723. ⁵Solar System Expl. Div., NASA GSFC, Greenbelt, MD 20771. ⁶Inst. of Planetary Research-DLR, D-12489 Berlin, Germany. ⁷Dept. of Terrestrial Magnetism, Carnegie Inst. of Washington, Washington, DC 20015. ⁸LPL, Univ. of Arizona, Tucson, AZ 85719. ⁹China Univ. of Geosciences (Wuhan), Wuhan, Hubei, P. R. China, 430074. ¹⁰Dept. of Earth, Atmos. & Planet. Sci., MIT, Cambridge, MA 02139.

Introduction: The distribution and geological history of large impact basins (diameter $D \geq 300$ km) on Mercury is important to understanding the planet's stratigraphy and surface evolution. It is also informative to compare the density of impact basins on Mercury with that of the Moon to understand similarities and differences in their impact crater and basin populations [1, 2].

A variety of impact basins were proposed on the basis of geological mapping with Mariner 10 data [e.g. 3]. This basin population can now be re-assessed and extended to the full planet, using data from the MErcury Surface, Space ENvironment, GEOchemistry, and Ranging (MESSENGER) spacecraft. Note that small-to-medium-sized “peak-ring” basins on Mercury are being examined separately [4, 5]; only the three largest peak-ring basins on Mercury overlap with the size range we consider here.

In this study, we (1) re-examine the large basins suggested on the basis of Mariner 10 data, (2) suggest additional basins from MESSENGER's global coverage of Mercury, (3) assess the size-frequency distribution of mercurian basins on the basis of these global observations and compare it to the Moon, and (4) analyze the implications of these observations for the modification history of basins on Mercury.

Data and Methodology: The primary dataset for this study consists of images and stereo topography from the Mercury Dual Imaging System (MDIS), supplemented with topography from the Mercury Laser Altimeter (MLA). Images from the first solar day of MESSENGER orbital operations provide nearly global coverage with imaging conditions optimized for morphology; these images have been mosaicked into a 250 m/px dataset. Additional data from MESSENGER and Mariner 10 flybys were examined when they provided improved coverage or resolution, and to compare with earlier interpretations. All data were imported and analyzed in ArcMap.

Basins were mapped systematically by repeat surveying of the MESSENGER image basemap at 1:5 and 1:2.5 million scales. We also specifically re-examined basins suggested in earlier studies of Mariner 10 and terrestrial radar images [3, 6, 7]. For both previously

suggested and newly mapped basins, a qualitative confidence was assigned based on the completeness of the basin rim as well as evidence such as ejecta, structure, or topography. Basins were assigned into “certain,” “probable,” or “suggested/unverified” classes; these assignments are conservative in that virtually all certain basins exist and their size estimates and locations are not likely to change. Many probable basins are also likely to exist, although they are more degraded. Basins classified as suggested/unverified are ambiguous; a substantial percentage are likely not to exist, although some may represent the location of the most highly degraded ancient basins.

Results: Distribution: The distribution of large basins mapped to date as certain (green) and probable (yellow) are shown in Fig. 1; 34 basins fit into these categories. An additional 18 basins (not shown) have been suggested but are not verified in present data.

The distribution of basins appears non-uniform (Fig. 1). One hypothesis for this observation is lateral variations in basin formation rates [8]. Other hypotheses remain open: (1) observational effects, which make recognition of degraded basins challenging, or (2) differential resurfacing, since many of the areas (e.g., west of Caloris) that have few apparent basins are covered by smooth or intercrater plains that may have erased the pre-existing basin population. Additional data from MESSENGER will help to resolve this question, particularly when global topography derived from stereo imaging is available.

Density of Mercurian Basins: Flyby data suggested that Mercury had close to the same density of large craters and small basins as the Moon in the diameter range $D \sim 128$ -512 km [1]. Our new data constitute a global dataset which allows a similar comparison of the density of large basins on the Moon and Mercury. Despite the density similarity for smaller-sized features, which appears to remain robust, the density of basins with $D \geq 500$ km appears substantially different (Fig. 2). The number of certain or probable basins with $D \geq 500$ km normalized to an area (A) of 10^6 km² is $N_{\text{Moon}}(500) = 0.37 \pm 0.1$ on the Moon and on Mercury is $N_{\text{Mercury}}(500) = 0.15 \pm 0.04$ (error bars are $\pm \sqrt{n/A}$, where n is number of basins).

We continue to entertain multiple hypotheses for this apparent difference, which has been suggested [9] and disputed [3] before. Possible explanations include (1) that the difference is an observational effect, (2) that fewer large basins formed on Mercury than the Moon, perhaps as a result of differences in impact conditions, (3) that basins on Mercury are not as topographically prominent as on the Moon and thus more readily subdued or buried, and (4) that basins experienced more resurfacing on Mercury than on the Moon.

Basin Resurfacing on Mercury: All of the large basins mapped to date are at least partially superposed by smooth plains, and the degree of basin flooding appears more substantial than is typical of basins on the Moon. From crater statistics, these plains are often substantially younger than the basins upon which they are superposed, so this association should not be taken as requiring a relationship between basin formation and plains emplacement. In addition, it appears that basins of comparable superposed crater density on the Moon (e.g., Nectaris, $N(20)=135\pm 14$ [10]) and on

Mercury (e.g., Sobkou, $N(20)=144\pm 31$) are commonly at substantially different degradation states (e.g., Fig. 3), with basins on Mercury having more poorly preserved rims, interior rings, and sculptured ejecta. Although more data are necessary to confirm this observation on a global basis, further elucidating the processes resulting in the distinct characteristics of large basins on Mercury will help us better understand its geological and geophysical evolution.

References: [1] Fassett, C.I. et al. (2011), *GRL*, 38, L10202. [2] Strom, R.G. et al. (2011), *PSS*, 59, 1960–1967. [3] Spudis, P.D and Guest, J.E. (1988), *Mercury*, Univ. Ariz. Press, 118–164. [4] Baker, D.M.H. et al. (2011) *PSS*, 59, 1932–1948. [5] Prockter, L.M. et al. (2012), *LPS*, 43, this meeting. [6] Butler, B.J. et al. (1993), *JGR*, 98, 15003–15023. [7] Ksanfomality, L.V. (2004), *Solar Syst. Res.*, 38, 21–27. [8] Wieczorek, M.A. et al. (2012), *Nature Geosci.*, 5, 18–21. [9] Frey, H. and Lowry, B.L. (1979), *Proc. LPSC*, 10, 2669–2687. [10] Fassett, C.I. et al. (2012), *JGR*, in press, 10.1029/2011JE003951.

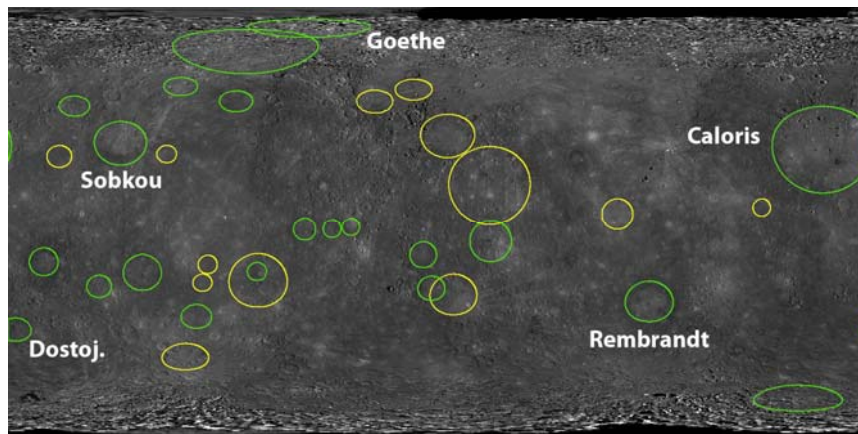


Figure 1. Certain (green) and probable (yellow) basins with $D \geq 300$ km on Mercury inferred from the first Mercury solar day of imaging.

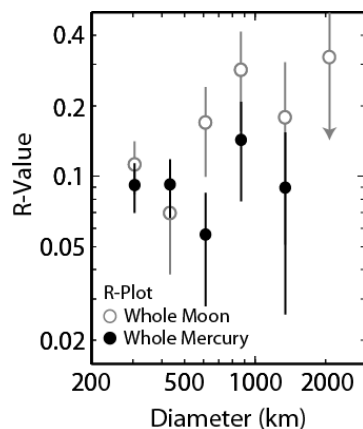


Figure 2. R plot showing the relative densities of certain and probable basins on the Moon and Mercury; for basins with $D \sim 128$ to 512 km, densities are similar, but for $D \geq 500$ km, there are far more basins per area recognized on the Moon than on Mercury. The largest bin on the Moon has $n=1$ (SPA), so the lower error bar is unbounded (arrow).

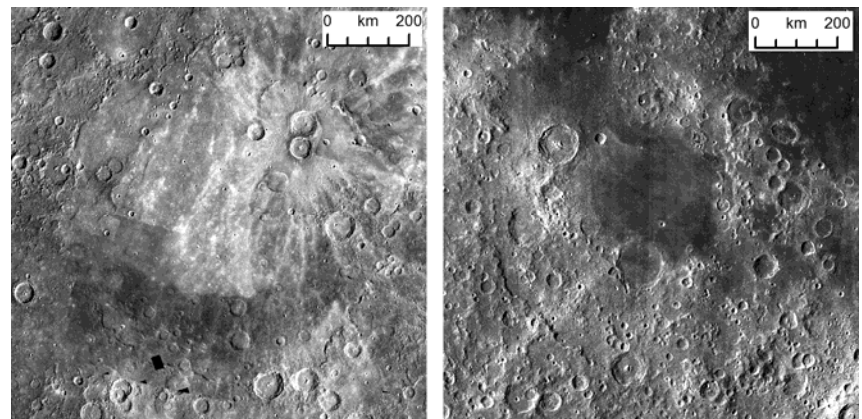


Figure 3. Sobkou basin ($D=770$ km) on Mercury (left) and Nectaris basin ($D=850$ km) on the Moon (right). Although both have been partially resurfaced by volcanic plains, Nectaris has a clear interior ring, discontinuous but sharp rim scarp, and visible sculptured ejecta. Sobkou has a far more subdued rim, no obvious interior ring, and no mappable ejecta. Sobkou image from MDIS global mosaic and Nectaris image from Lunar Reconnaissance Orbiter Camera wide-angle camera global mosaic.